Transition Metal Complexes Coupled to Vacancies in Oxides: Origin of Different Properties of Cr3+ in MgO Bounded to a < 100 > or < 110 > Mg2+ Vacancy

ARTICLE *in* THE JOURNAL OF PHYSICAL CHEMISTRY A · OCTOBER 2013

Impact Factor: 2.69 · DOI: 10.1021/jp409276p · Source: PubMed

4 AUTHORS, INCLUDING:

Miguel Moreno
Universidad de Cantabria
224 PUBLICATIONS **2,712** CITATIONS

SEE PROFILE

THE JOURNAL OF PHYSICAL CHEMISTRY A

Article

pubs.acs.org/JPCA

Transition Metal Complexes Coupled to Vacancies in Oxides: Origin of Different Properties of Cr^{3+} in MgO Bounded to a ⟨100⟩ or ⟨110⟩ Mg^{2+} Vacancy

J. A. Aramburu,*[,†] P. García-Fernández,[†] M. T. Barriuso,[‡] and M. Moreno[†]

[†]Departamento de Ciencias de la Tierra y Física de la Materia Condensada, Universidad de Cantabria, Avenida de los Castros s/n, 39005 Santander, Spain

[‡]Departamento de Física Moderna, Universidad de Cantabria, Avenida de los Castros s/n, 39005 Santander, Spain

ABSTRACT: Despite the importance of vacancies over the properties of insulating oxides its influence on neighboring transition metal ions is far from being understood. This work is devoted to find the origin of various up to now unexplained properties of chromium bounded either to a ⟨100⟩ or a ⟨110⟩ Mg^{2+} vacancy in MgO. In these model systems particular attention is paid to understand, by means of ab initio calculations, why the cubic field splitting parameter, 10Dq, is surprisingly 1600 cm^{-1} higher for a ⟨100⟩ than for a ⟨110⟩ vacancy, a fact behind the suppression of the sharp $^2E \rightarrow {}^4A_2$ luminescence in the latter case. Our calculations, which reproduce the main experimental facts, prove that the average $Cr^{3+}-O^{2-}$ distance is the same within 0.8% for both systems, and thus, the low 10Dq value for a ⟨110⟩ vacancy is shown to be due mainly to the electrostatic potential from the missing Mg^{2+} ion, which increases the energy of antibonding t_{2g} ($\sim xy, xz, yz$) levels. By contrast, for a ⟨100⟩ Mg^{2+} vacancy that potential provides a supplementary increase of the e_g ($\sim x^2 - y^2, 3z^2 - r^2$) level energy and thus of 10Dq. The existence of the $^2E \rightarrow {}^4A_2$ luminescence for Cr^{3+}-doped MgO under perfect cubic symmetry or with a ⟨100⟩ vacancy is shown to be greatly helped by the internal electric field created by the rest of the lattice ions on the CrO_6^{9-} unit, whose importance is usually ignored. The present results underline the role of ab initio calculations for unveiling the subtle effects induced by a close vacancy on the properties of transition metal ions in oxides. At the same time they stress the failure of the empirical superposition model for deriving the equilibrium geometry of C_{4v} and C_{2v} centers in MgO:Cr^{3+}.

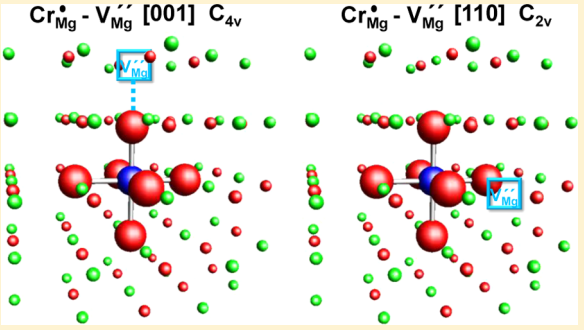

1. INTRODUCTION

Metal oxides have a large importance in modern technology as they appear in energy generators, transparent conductors, superconductors, giant magnetoresistive materials, multiferroics, solid state ionics, or catalysts, just to mention a few examples. Moreover, their properties can be tuned or completely transformed upon doping, either with impurities or the appearance of vacancies in the bulk or in the surface during the growth process.[1−4] Specifically, the introduction of charge into an oxide lattice through physical or chemical means may activate strong Coulomb and exchange interactions that can spontaneously break the point symmetry of the solid, creating exotic quantum liquid phases such as high temperature superconductors and metallic non-Fermi liquids.[5] Also the magnetic properties of materials like CaO,[6,7] HfO_2,[8] Mn-doped ZnO,[9] or Nb-doped $SrTiO_3$[10] indicate that vacancies in the lattice deeply modify their properties. These defects have also important structural effects as, for example, in the case of the TiO_2 surface,[11] influencing reactivity. Similarly the properties of oxide heterostructures that show great promise in electronics, like the interface between $SrTiO_3$ and $LaAlO_3$ insulators, are determined, to a large degree, by defects. In fact, several works argue that the metallic state in this system is due to vacancies appearing during the lattice growth process.[12,13]

In spite of their evident importance described above, it is often not simple to experimentally characterize vacancies and, especially, to understand in detail the effect they have on the surrounding ions. Along this line it is particularly interesting the study of *model* systems that could provide some light on how to deal with more involved cases. This work is precisely addressed to clarify puzzling features concerning two model systems formed in the MgO *cubic* lattice doped with Cr^{3+} impurities that enter the lattice substituting Mg^{2+} ions. In MgO:Cr^{3+}, aside from the existence of perfect octahedral CrO_6^{9-} complexes (cubic centers, called $Cr_{Mg}^{\bullet}$ in the Kröger−Vink notation), electron paramagnetic resonance (EPR) and optical data *suggest* the formation of other two centers involving the same complex but attached to a close Mg^{2+} vacancy (V_{Mg}'', in the Kröger−Vink notation), in different positions.[14−20] The proposed structure for such $Cr_{Mg}^{\bullet} - V_{Mg}''$ centers is depicted in Figure 1. In one case V_{Mg}'' appears in the nearest position to $Cr_{Mg}^{\bullet}$ along a ⟨110⟩

Received: September 17, 2013
Revised: October 28, 2013
Published: October 28, 2013

   dx.doi.org/10.1021/jp409276p | J. Phys. Chem. A 2013, 117, 12642−12647

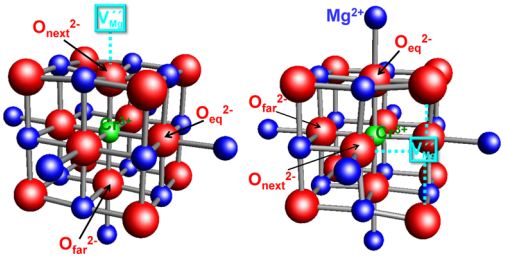

Figure 1. Structures of the C_{4v} (left) and C_{2v} (righ) $Cr_{\dot{M}g} - V_{Mg}''$ centers in MgO:Cr^{3+}.

direction (C_{2v} symmetry), while in the other center the vacancy replaces a closest Mg^{2+} ion along a ⟨100⟩ direction (C_{4v} symmetry). Despite that these C_{2v} and C_{4v} model centers, together with the cubic center formed in MgO:Cr^{3+}, have widely been investigated experimentally, there are still three relevant issues that remain to be clarified. (i) As vacancies are not *directly* identified by means of EPR and optical techniques, it is thus necessary to confirm that both C_{4v} and C_{2v} centers actually involve a vacancy and not any impurity attached to the CrO_6^{9-} complex. (ii) A microscopic insight into the properties exhibited by model C_{4v} and C_{2v} centers requires knowing the actual local relaxation on the CrO_6^{9-} complex induced by the bounded defect. This relevant issue has hitherto been explored only through Hartree−Fock calculations[21] and the empirical superposition model.[22] As there are significant differences between both results an ab initio study could help to clear out this matter. (iii) As a salient feature the optical excitation spectra prove that the energy maximum of the $^4A_2(t_{2g}^3) \rightarrow {}^4T_2(t_{2g}^2e_g^1)$ band (corresponding to the so-called cubic field splitting parameter of the ligand field theory, 10Dq) of C_{4v} and C_{2v} $Cr_{\dot{M}g} - V_{Mg}''$ centers is shifted in a different way with respect to that for the cubic center.[14,16−18] More precisely, the experimental value for the cubic center is $10Dq(O_h)$ = 16300 cm^{-1}, while that for the tetragonal center is a little higher, $10Dq(C_{4v})$ = 16900 cm^{-1}, and that for the rhombic center certainly smaller, $10Dq(C_{2v})$ = 15260 cm^{-1}. No explanation on this surprising fact has been reported up to now.

It is worth noting now that, with respect to $10Dq(O_h)$ = 16300 cm^{-1}, the shift in the maximum of the $^4A_2(t_{2g}^3) \rightarrow {}^4T_2(t_{2g}^2e_g^1)$ band of −1040 cm^{-1} assigned to the presence of a close vacancy along ⟨110⟩ is *also* responsible for the surprising absence of the sharp $^2E \rightarrow {}^4A_2$ emission for the C_{2v} center. In fact, this sharp emission is characteristic of Cr^{3+} in oxides like ruby, emerald, or alexandrite[14,23] and is observed for both the cubic and C_{4v} centers in MgO:Cr^{3+} at 14320 and 14250 cm^{-1}, respectively.[14−20] By contrast, the value $10Dq(C_{2v})$ = 15260 cm^{-1} and a Stokes shift for the $^4A_2(t_{2g}^3) \rightarrow {}^4T_2(t_{2g}^2e_g^1)$ transition of Cr^{3+} ions in oxides around 2500 cm^{-1}[14,21] favor a luminescence from the $^4T_2(t_{2g}^2e_g^1)$ state for the C_{2v} center giving rise to a broad band peaked at 12500 cm^{-1}.[14,16,18]

Seeking to clear up all these relevant issues, ab initio periodic and cluster calculations have been carried out on the model C_{4v} and C_{2v} $Cr_{\dot{M}g} - V_{Mg}''$ centers formed in MgO:Cr^{3+}. It should be stressed that the calculations of insulating systems with transition metal cations become more complex when there are vacancies as they lower the symmetry, and thus, bigger supercells and clusters have to be employed.[24−26] Owing to this fact only one nonempirical theoretical work on C_{4v} and C_{2v} $Cr_{\dot{M}g} - V_{Mg}''$ centers in MgO:Cr^{3+} has been reported.[21] However, in that calculation, performed at the Hartree−Fock level, the different optical spectrum displayed by such centers is not investigated. This situation thus differs from that for the cubic center formed in MgO:Cr^{3+}, which, by virtue of its relative simplicity, has been explored theoretically in more detail.[21,27−29]

For achieving the present goals, ab initio periodic calculations have first been carried out in order to determine the *actual* local lattice distortion induced by the V_{Mg}'' vacancy in both C_{4v} and C_{2v} centers. In a second step, the 10Dq values for the two $Cr_{\dot{M}g} - V_{Mg}''$ centers formed in MgO:Cr^{3+} have been calculated following the same procedure previously employed for the cubic center.[27] Particular attention is paid to see whether the calculated 10Dq values are consistent with experimental findings. Unfortunately, the splitting expected in the $^4A_2(t_{2g}^3) \rightarrow {}^4T_2(t_{2g}^2e_g^1)$ band for C_{4v} and C_{2v} centers is not well resolved experimentally, due to a bandwidth around 2000 cm^{-1}.[14,16,18]

As active electrons are *essentially localized* in the CrO_6^{9-} unit, it has already been shown for the cubic center that 10Dq can be understood just considering the complex subject to the electrostatic potential, $V_R(\mathbf{r})$, created by the rest of lattice ions.[27] Although, owing to symmetry of the O_h center, $V_R(\mathbf{r})$ is constant around the Cr^{3+} site, this is no longer true in the region closer to ligands, and thus, $V_R(\mathbf{r})$ gives rise to an extrinsic contribution, Δ_R, to 10Dq, which has to be added to the intrinsic one, $(10Dq)_i$, calculated for the *isolated* CrO_6^{9-} unit. Thus, the final 10Dq value for the cubic center is simply given by[27]

$$10Dq = (10Dq)_i + \Delta_R \quad (1)$$

This expression points out that the 10Dq value of transition metal complexes embedded in insulating host lattices cannot be understood considering *only* the isolated complex although $\Delta_R/(10Dq)_I \approx 10\%$ for ruby[30,31] or the cubic center in MgO:Cr^{3+}.[27] Thus, while the spectrochemical series or the dependence of 10Dq upon the metal−ligand distance, R, are mainly determined by $(10Dq)_i$,[32] the different color displayed by ruby and emerald is essentially governed by the extrinsic Δ_R contribution.[30,31] As an exception, lattices with normal perovskite structure give rise to a $V_R(\mathbf{r})$ essentially flat in the complex region, and thus, 10Dq practically arises from the intrinsic contribution.[33,34]

The present work is arranged as follows. An account of computational methods employed in the present work is given in section 2, while main results are displayed and discussed in section 3. Some final remarks are provided in the last section.

2. COMPUTATIONAL DETAILS

For determining the equilibrium geometry of C_{4v} and C_{2v} $Cr_{\dot{M}g} - V_{Mg}''$ centers in MgO:Cr^{3+}, periodic supercell calculations based on the density functional theory (DFT) have been carried out by means of the CRYSTAL package that employs localized Gaussian basis-sets to represent the Bloch orbitals.[35] All ions have been described by all-electron basis-sets of reasonably high quality (8−511G* for Mg, 8−411G* for O, and 86−411G** for Cr) taken from the CRYSTAL database.[36] Calculations have been performed on supercells where the Cr^{3+} impurity replaces a Mg^{2+} ion with a close V_{Mg}'' in ⟨100⟩ or ⟨110⟩ directions (Figure 1). For both C_{4v} and C_{2v} centers the charge neutrality is achieved through a $+e$ charge homogenously distributed in the supercell. In the case of the C_{4v} center, a 2 × 2 × 3 supercell involving 95 ions has been used in our calculations, while a bigger 3 × 2 × 3 supercell of 142 ions for the C_{2v} center with lower symmetry. We have treated the

dx.doi.org/10.1021/jp409276p | J. Phys. Chem. A 2013, 117, 12642−12647

exchange and correlation of the electrons through two different functionals: PBEsol designed specifically to improve the generalized gradient approximation (GGA) in solids,[37] and the B1WC hybrid functional[38] that allows one to obtain geometries and band gaps with great accuracy and reliability.

As the ability of the CRYSTAL program to treat excited states is very limited, we have calculated the value of the cubic-field splitting parameter, 10Dq, for the two $Cr_{\dot{M}g} - V''_{Mg}$ centers following the same procedure already employed for the cubic center in MgO:Cr^{3+}.[27] So, we have used a cluster approach, by means of the Amsterdam density functional (ADF) code,[39] performing DFT calculations for an average configuration where the three unpaired 3d(Cr) electrons have been equally distributed among the five antibonding orbitals.[40] Calculations have been performed for the CrO_6^{9-} complex in vacuo, at the corresponding equilibrium geometry computed in the supercell calculations, and also considering an embedding of about 200 point charges previously fitted in order to reproduce the right $V_R(\mathbf{r})$ potential coming from all ions of the MgO crystal lying outside the CrO_6^{9-} unit.[27,31] The exchange-correlation energy was computed according to the Perdew–Wang-91 functional in the GGA.[41]

3. RESULTS AND DISCUSSION

Optimized geometries calculated in the C_{4v} $Cr_{\dot{M}g} - V''_{Mg}$ center by means of the GGA-PBEsol and hybrid-B1WC functionals are very similar, as shown in Table 1, and reflect the existence

Table 1. Values of the Equilibrium Cr^{3+}–O^{2-} Distances Computed for the C_{4v} $Cr_{\dot{M}g} - V''_{Mg}$ Center Formed in MgO:Cr^{3+} Using a 2 × 2 × 3 Supercell with 95 Ions and Two Different Functionals; in Addition to R_{next}, R_{eq} and R_{far} Reflecting the Distances between Cr^{3+} and the O_{next}^{2-}, O_{eq}^{2-}, and O_{far}^{2-} Ligands in Figure 1, the Value of the Average Cr^{3+}–O^{2-} Distance, $\langle R\rangle$, Is Also Reported; the Number of Ligands in Next, Equatorial, and Far Positions for the C_{4v} Center Is Also Given in Parentheses; All Distances Are in pm

functional	R_{next} (1×)	R_{eq} (4×)	R_{far} (1×)	$\langle R\rangle$
GGA-PBE	191.7	204.0	204.6	202.1
hybrid-B1WC	191.2	203.6	204.0	201.6

of a significant local ligand relaxation due to the ⟨100⟩ V''_{Mg} vacancy. So, compared to the Cr^{3+}–O^{2-} distance calculated[27] for the cubic center (R_c = 202.9 pm) that corresponding to the closest ligand to the vacancy, O_{next}^{2-} (Figure 1), termed R_{next}, is reduced by 5.8%. By contrast, R_{eq} and R_{far}, related to the four equatorial ligands, O_{eq}^{2-}, and the far ligand, O_{far}^{2-}, respectively (Figure 1), experience an increase but smaller than 1%. This situation is thus similar to that found for the $Cr_{\dot{M}} - V''_{M}$ centers in KMF_3:Cr^{3+} (M = Mg, Zn) where the V''_M vacancy lies on the closest M^{2+} ion to chromium ion along ⟨001⟩, and thus, V''_M, the ligand F_{next}^- and Cr^{3+} ion are all on the same line.[24] As to the average Cr^{3+}–O^{2-} distance, $\langle R\rangle$, for the C_{4v} $Cr_{\dot{M}g} - V''_{Mg}$ center, it is found to be equal to 201.6 pm, and thus, very close to R_c = 202.9 pm calculated for the cubic center.

A somewhat different situation is found for the equilibrium geometry of the C_{2v} $Cr_{\dot{M}g} - V''_{Mg}$ center (Figure 1) where the V''_{Mg} vacancy, O_{next}^{2-}, and Cr^{3+} ions are not aligned. Indeed, R_{next} = 198.5 pm (Table 2), which is only 2.2% smaller than R_c = 202.9 pm, characteristic of the cubic center, while the Cr^{3+}–O^{2-} distance for the two far ligands is found to be R_{far} = 208.3 pm, thus giving rise to $\langle R\rangle$ = 203.3 pm, which is only 0.8% higher than that for the C_{4v} center.

Table 2. Values of the Equilibrium R_{next}, R_{eq}, and R_{far} Distances Calculated for the C_{2v} $Cr_{\dot{M}g} - V''_{Mg}$ Center Formed in MgO:Cr^{3+} Using a 3 × 2 × 3 Supercell with 142 Ions and Two Different Functionals, Together with the Value of the Average Cr^{3+}–O^{2-} Distance, $\langle R\rangle$; the Number of Ligands in Next, Equatorial and Far Positions for the C_{2v} Center Is Also Given in Parentheses; All Distances Are in pm

functional	R_{next} (2×)	R_{eq} (2×)	R_{far} (2×)	$\langle R\rangle$
GGA-PBEsol	198.6	203.6	209.0	203.7
hybrid-B1WC	198.5	203.1	208.3	203.3

The equilibrium geometry of both C_{4v} and C_{2v} $Cr_{\dot{M}g} - V''_{Mg}$ centers was early derived using a Hartee–Fock calculation on a simple CrO_6^{9-} unit, while the rest of the lattice is simulated by means of a classical shell model.[21] The results derived from such an approach for the C_{4v} center (R_{next} = 192 pm, R_{eq} = 203 pm, and R_{far} = 204 pm) and the C_{2v} center (R_{next} = 199 pm, R_{eq} = 204 pm, and R_{far} = 206 pm) are thus close to those obtained in the present work (Tables 1 and 2), especially for the former center. A quite different situation appears, however, when comparing the results of Tables 1 and 2 with those derived from the experimental zero-field splitting *assuming* the validity of the empirical superposition model. So, the values R_{next} = 177 pm, R_{eq} = 194 pm, and R_{far} = 202.8 pm reported by Yeung for the C_{4v} center[22] using that procedure imply $R_{next} - R_{far}$ = 25.8 pm, a figure that is practically *twice* that found in the present ab initio calculations. The strong assumptions and limitations behind the empirical superposition model are discussed in ref 42.

Let us now focus on the 10Dq values for the O_h, C_{4v}, and C_{2v} centers formed in MgO:Cr^{3+} calculated in the present work. Despite its relevance, the optical properties of C_{4v} and C_{2v} $Cr_{\dot{M}g} - V''_{Mg}$ centers are not explored at all in the previous work by Groh et al.[21] Results for the cubic center are given in Table 3

Table 3. Calculated 10Dq Values (in cm^{-1}) for the Cubic Center Formed in MgO:Cr^{3+} at Three Different Values of the Cr^{3+}–O^{2-} Distance, R (in pm)[a]

	10Dq	
R	isolated	adding $V_R(\mathbf{r})$
201.6	14850	16616
202.9	14454	16236
203.3	14333	16027

[a]The value R_c = 202.9 pm is the equilibrium distance computed for the cubic center, while R = 201.6 and 203.3 pm correspond to the average Cr^{3+}–O^{2-} distance, $\langle R\rangle$, calculated for the C_{4v} and C_{2v} $Cr_{\dot{M}g} - V''_{Mg}$ centers, respectively, by means of the hybrid functional. For every R value the 10Dq value calculated for the isolated CrO_6^{9-} unit and including the effect of the electrostatic potential, $V_R(\mathbf{r})$, are both reported. The experimental 10Dq value measured for the cubic centre is equal to 16150 cm^{-1}.[16]

while those for the two $Cr_{\dot{M}g} - V''_{Mg}$ centers are reported in Table 4. It can be noticed that the calculated 10Dq values at the right equilibrium geometry reasonably reproduce the experimental findings for the three centers. These facts thus strongly support the structure previously proposed for the C_{4v} and C_{2v} centers (Figure 1), and thus the low symmetry seen in EPR

dx.doi.org/10.1021/jp409276p | J. Phys. Chem. A 2013, 117, 12642–12647

Table 4. Calculated versus Experimental 10Dq Values (in cm^{-1}) for C_{4v} and C_{2v} $Cr_{\dot{M}g} - V''_{Mg}$ Centers in MgO:Cr^{3+}[a]

		10Dq				
center	⟨R⟩	(a) isolated	(b) $+V_R(\mathbf{r})$ without vacancy	(c) $+V_R(\mathbf{r})$ with vacancy	exptl	refs
C_{4v}	201.6	14874	16648	16866	16900	14, 16−18
C_{2v}	203.3	14285	16059	15438	15260	14, 16−18

[a]Calculated values have been computed for a distorted CrO_6^{9-} complex at the equilibrium geometries optimized in the periodic calculations (with mean ⟨R⟩ Cr^{3+}−O^{2-} distances, given in pm units) in three successive steps: (a) isolated complex; (b) adding the $V_R(\mathbf{r})$ potential corresponding to the perfect MgO lattice (that is, without vacancies); (c) the same as in b but finally placing the V''_{Mg} vacancy in the position of closest ⟨001⟩ or ⟨110⟩ Mg^{2+} cations, respectively. Thus, in this last step, the effect of the electrostatic potential induced by the vacancy, $V_v(\mathbf{r})$, is considered.

spectra[14,15] is in fact due to the presence of a close V''_{Mg} vacancy attached to a CrO_6^{9-} complex.

Once this relevant matter is cleared out it is necessary to understand why a ⟨110⟩ V''_{Mg} vacancy gives rise to a decrease of 10Dq, while this quantity increases when the vacancy is located along ⟨100⟩. In particular, it is quite important to clarify whether the different 10Dq value exhibited by the C_{4v} and C_{2v} centers is only the result of a different ⟨R⟩ value.

Seeking to answer these questions, we have first calculated the variation of 10Dq for the cubic center around R_c = 202.9 pm. As shown in Table 3 an increase of 0.8% in the Cr^{3+}−O^{2-} distance, R, of this center gives rise to a decrease of 10Dq of only 600 cm^{-1}. This variation just reflects the 10Dq sensitivity of octahedral complexes to R changes, essentially due to the intrinsic contribution, a matter discussed in ref 32. Nevertheless, the 600 cm^{-1} variation of 10Dq when changing R of the cubic center by 0.8% is certainly smaller than the experimental $10Dq(C_{4v}) - 10Dq(C_{2v})$ = 1600 cm^{-1} measured[16−18] for the two $Cr_{\dot{M}g} - V''_{Mg}$ centers. This fact strongly suggests that the quantity $10Dq(C_{4v}) - 10Dq(C_{2v})$ can hardly be understood considering *only* the average Cr^{3+}−O^{2-} distance, ⟨R⟩, of both centers.

Seeking to shed light on this relevant issue, we have calculated the 10Dq value of C_{4v} and C_{2v} centers in three steps using *in all cases* the equilibrium geometries reported in Tables 1 and 2. In a first step, 10Dq has been calculated for the distorted CrO_6^{9-} unit but discarding the effects of $V_R(\mathbf{r})$ upon 10Dq. In a second step, the effects of $V_R(\mathbf{r})$ upon 10Dq are considered but ignoring the presence of the V''_{Mg} vacancy. This means that the contribution of closest ⟨001⟩ or ⟨110⟩ Mg^{2+} cations is *artificially* incorporated into $V_R(\mathbf{r})$. In the last step, such ions are of course removed for calculating the *right* $V_R(\mathbf{r})$ in the two considered $Cr_{\dot{M}g} - V''_{Mg}$ centers. As shown in Table 4 the calculated 10Dq values for both centers in the first and second steps are very close to those derived for the cubic center (Table 3) at distances R = 201.6 and 203.3 pm. Therefore, in the first two steps, 10Dq essentially reflects the slightly different ⟨R⟩ value of two $Cr_{\dot{M}g} - V''_{Mg}$ centers but *only* 35% of the experimental $10Dq(C_{4v}) - 10Dq(C_{2v})$ = 1640 cm^{-1} is then accounted for. As shown in Table 4, this situation is substantially improved when the presence of the close V''_{Mg} vacancy in both C_{4v} and C_{2v} centers is incorporated into the calculation of the electrostatic potential $V_R(\mathbf{r})$. Indeed, 10Dq of the C_{2v} center undergoes a *supplementary* decrease of 620 cm^{-1}, while there is an increase of 220 cm^{-1} for the tetragonal center, and thus, the calculated value $10Dq(C_{4v}) - 10Dq(C_{2v})$ = 1330 cm^{-1} is now much closer to the experimental figure. This result thus stresses that the *variation* of the electrostatic potential $V_R(\mathbf{r})$ induced by the vacancy, called $V_v(\mathbf{r})$, plays a key role for understanding the shift in 10Dq experienced by the two C_{4v} and C_{2v} centers.

The quantity $(-e)V_v(\mathbf{r})$, reflecting directly the energy felt by an electron of the CrO_6^{9-} unit due to the presence of the electrostatic potential associated with the vacancy for both C_{4v} and C_{2v} centers, is depicted in Figure 2. It can be noticed that

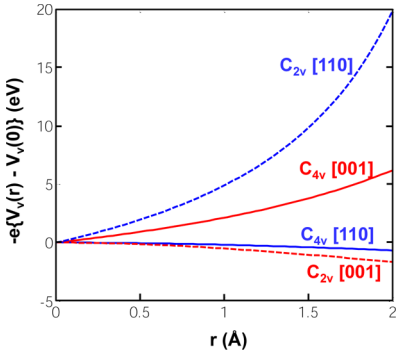

Figure 2. Picture of the $(-e)\{V_v(\mathbf{r}) - V_v(0)\}$ potential energy for both C_{4v} and C_{2v} $Cr_{\dot{M}g} - V''_{Mg}$ centers, where $V_v(\mathbf{r})$ means the contribution of the V''_{Mg} vacancy to the electrostatic potential $V_R(\mathbf{r})$ felt by an electron of the CrO_6^{9-} unit. Energy is depicted along [001] and [110] directions for both centers.

$(-e)\{V_v(\mathbf{r}) - V_v(0)\}$ is clearly higher for the C_{2v} center when **r** is parallel to ⟨110⟩ than for the C_{4v} center when **r** is along ⟨001⟩. This fact is fully consistent with a smaller distance between the vacancy and the Cr^{3+} impurity for the former center. Moreover, when **r** runs perpendicular to the Cr^{3+}−V''_{Mg} line, the variation of $V_v(\mathbf{r})$ is, as expected, much smaller than when it moves along such a line.

Therefore, the contribution of $V_v(\mathbf{r})$ to $V_R(\mathbf{r})$ induces an *extra increase* of the $t_{2g}(xy)$ level energy of the C_{2v} center. As this level is lying *below* the $e_g(3z^2 - r^2, x^2 - y^2)$ level under octahedral coordination, it favors a decrease of 10Dq, a fact consistent albeit qualitatively, with the experimental results gathered in Table 4 for such a center. Along this line also the $V_v(\mathbf{r})$ contribution for the C_{4v} center increases the energy of the $e_g(3z^2 - r^2)$ orbital pointing toward the ⟨001⟩ direction. Nevertheless, as e_g levels are lying above t_{2g} levels, the addition of $V_v(\mathbf{r})$ gives rise to a supplementary increase of 10Dq for the C_{4v} center and thus explains qualitatively the experimental results (Table 4). Moreover, as the effects of $V_v(\mathbf{r})$ are stronger for the C_{2v} than for the C_{4v} center (Figure 2), it is now understandable why $V_v(\mathbf{r})$ leads to an increase of only 200 cm^{-1} for the C_{4v} center, while the decrease induced on the C_{2v} center (600 cm^{-1}) is certainly much bigger.

The present results prove that 10Dq for the two $Cr_{\dot{M}g} - V''_{Mg}$ centers formed in MgO:Cr^{3+} can essentially be understood through the average Cr^{3+}−O^{2-} distance, ⟨R⟩, of the CrO_6^{9-} unit and the right $V_R(\mathbf{r})$ potential, where the contribution of the V''_{Mg} vacancy, $V_v(\mathbf{r})$, plays an important role. It should be noted, however, that bigger changes are expected for properties with a much higher *local* character.[24] For instance, we have verified that for the C_{4v} center there is a significant difference between the Mulliken charge, q, corresponding to the O_{next}^{2-} ligand (q =

dx.doi.org/10.1021/jp409276p | J. Phys. Chem. A 2013, 117, 12642−12647

$-1.35e$) and that for O_{far}^{2-} ($q = -1.63e$). As such a difference is just the reflection of a distinct covalency in $Cr^{3+}-O_{next}^{2-}$ and $Cr^{3+}-O_{far}^{2-}$ bonds, this implies that the superhyperfine tensor for O_{next}^{2-} ligand is likely not to be the same as for the O_{far}^{2-} one. Although this conclusion has not been yet verified experimentally, as it requires working with MgO samples enriched with the ^{17}O isotope, it has been proved to be right for the similar $Cr_{\dot{Zn}} - V''_{Zn}$ center formed in $KZnF_3:Cr^{3+}$.[43,24] These results on Mulliken charges stress that the electronic density in the complex is significantly modified by the presence of a close vacancy.[24] The existence of this electronic relaxation is thus against the idea that ions can be considered as being stiff, and thus, its properties can easily be transferred from high symmetry to low symmetry systems, such as it is assumed in the empirical superposition model.[42]

4. FINAL REMARKS

The present results show the usefulness of ab initio calculations for exploring complex centers involving transition metal cations and close vacancies. On one hand, vacancies are not directly seen by EPR and the low symmetry of spectra could also be due to the presence of close impurities. Ab initio calculations are thus of great help for overcoming that dichotomy. Moreover, they provide with a reasonable picture of the local lattice relaxation around the transition metal cation. In the present study of C_{4v} and C_{2v} $Cr_{\dot{Mg}} - V''_{Mg}$ centers in $MgO:Cr^{3+}$, the obtained equilibrium distances stress once more the lack of reliability of conclusions reached through the empirical superposition model.[22] This model is based on strong assumptions whose validity is discussed in ref 42.

On the other hand, ab initio calculations have unveiled the subtle origin of different properties displayed by the model C_{4v} and C_{2v} $Cr_{\dot{Mg}} - V''_{Mg}$ centers formed in $MgO:Cr^{3+}$. which up to now remained unexplained. As a main conclusion it is proved that the differences in 10Dq depend on $\langle R \rangle$ but especially on the electrostatic potential created by the vacancy, $V_v(\mathbf{r})$, on the CrO_6^{9-} unit where active electrons are confined.

Although the presence of the V''_{Mg} vacancy induces a significant structural relaxation, nevertheless the $\langle R \rangle$ value for the C_{2v} center is found to be only 0.8% higher than that for the C_{4v} center and practically equal to the $Cr^{3+}-O^{2-}$ distance for the O_h center. Accordingly, the negative shift of 1000 cm^{-1} on passing from the O_h to the C_{2v} center is greatly due to the repulsive $V_v(\mathbf{r})$ potential along $\langle 110 \rangle$ directions. This negative shift in 10Dq favors the suppression of the sharp $^2E \rightarrow {}^4A_2$ emission for the C_{2v} center, while it remains in the case of O_h and C_{4v} centers such as it is observed experimentally.[14,16−18]

An interesting question is why in the experiments carried out on $MgO:Cr^{3+}$ *both* C_{4v} and C_{2v} centers are observed.[14−20] Some light on this issue can obtained from the recent calculations[25] carried out on V'_{Na} vacancy centers formed in $NaCl:M^{2+}$ (M = Rh, Ir, Mn). If we call $\Delta E(nn;nnn)$ the total energy difference corresponding to having a $\langle 110 \rangle$ V'_{Na} vacancy (nearest neighbor position) or a $\langle 100 \rangle$ one (next nearest neighbor position) the calculated $|\Delta E(nn;nnn)|$ values for the three divalent impurities are found to be *only* of the order of 0.01 eV.[25] The experimental $\Delta E(nn;nnn)$ value measured for $NaCl:Mn^{2+}$ has been reported to be either 0.034[44] or 0.043 eV.[45]

As a salient feature the present study proves that the electrostatic potential, $V_R(\mathbf{r})$, created by the rest of the lattice ions plays a key role for stabilizing ^2E as the first excited state for both O_h center and C_{4v} $Cr_{\dot{Mg}} - V''_{Mg}$ center formed in $MgO:Cr^{3+}$. Thus, the internal electric field associated with $V_R(\mathbf{r})$, usually ignored in the study of insulating compounds, is greatly responsible for the existence of $^2E \rightarrow {}^4A_2$ luminescence in the cubic center. Along this line, the different spectroscopic properties due to Cr^{3+} or Mn^{2+} impurities in the normal perovskite $KMgF_3$ and in the inverted perovskite $LiBaF_3$ just reflect the *different* shape of $V_R(\mathbf{r})$ in such cubic lattices.[46]

Obviously, the importance of internal electric fields is not restricted to doped compounds as they can also play a key role in pure insulating compounds where active electrons are thus localized.[47] For instance, a recent study[48] has proved that the $d_{x^2-y^2}-d_{3z^2-r^2}$ gap in the K_2CuF_4 pure compound is not entirely due to the local distortion around Cu^{2+}. Indeed about 25% of such a splitting is the result of the tetragonal internal electric field acting on a CuF_6^{4-} unit.

Furthermore, the shape of $V_R(\mathbf{r})$ has been shown to be quite important for understanding the actual *structure* of some Cu^{2+} compounds. For instance, the surprising compressed geometry observed for $K_2ZnF_4:Cu^{2+}$[49] has been proved to be greatly due to the form of the internal field in that layered perovskite.[50]

Further work on the influence of internal electric fields on the properties of insulating oxides and fluorides containing transition metal cations is under way.

AUTHOR INFORMATION

Corresponding Author

*(J.A.A.) E-mail: aramburj@unican.es. Phone: +34-942201507.

Notes

The authors declare no competing financial interest.

ACKNOWLEDGMENTS

The support by the Spanish Ministerio de Ciencia y Tecnología under Projects FIS2012-30996 and FIS2009-07083 is acknowledged.

REFERENCES

(1) Wendt, S.; Sprunger, P. T.; Lira, E.; Madsen, G. K. H.; Li, Z. S.; Hansen, J. O.; Matthiesen, J.; Blekinge-Rasmussen, A.; Laegsgaard, E.; Hammer, B.; et al. The Role of Interstitial Sites in the Ti3d Defect State in the Band Gap of Titania. *Science* **2008**, *320*, 1755−1759.

(2) McElroy, K.; Lee, J.; Slezak, J. A.; Lee, D. H.; Eisaki, H.; Uchida, S.; Davis, J. C. Atomic-Scale Sources and Mechanism of Nanoscale Electronic Disorder in $Bi_2Sr_2CaCu_2O_{8+\delta}$. *Science* **2005**, *309*, 1048−1052.

(3) Ohtomo, A.; Muller, D. A.; Grazul, J. L.; Hwang, H. Y. Artificial Charge-Modulation in Atomic-Scale Perovskite Titanate Superlattices. *Nature* **2002**, *419*, 378−380.

(4) Henrich, V. E. *The Surface Science of Metal Oxides*; Cambridge University Press: Cambridge, U.K., 1994.

(5) Kivelson, S. A.; Fradkin, E.; Emery, V. J. Electronic Liquid-Crystal Phases of a Doped Mott Insulator. *Nature* **1998**, *393*, 550−553.

(6) Elfimov, I. S.; Yunoki, S.; Sawatzky, G. A. Possible Path to a New Class of Ferromagnetic and Half-Metallic Ferromagnetic Materials. *Phys. Rev. Lett.* **2002**, *89*, 216403−216406.

(7) Errico, L. A.; Rentería, M.; Weissmann, M. Theoretical Study of Magnetism in Transition-Metal-Doped TiO_2 and $TiO_{2-\delta}$. *Phys. Rev. B* **2005**, *72*, 184425−184433.

(8) Venkatesan, M.; Fitzgerald, C. B.; Coey, J. M. D. Thin Films: Unexpected Magnetism in a Dielectric Oxide. *Nature* **2004**, *430*, 630.

(9) Sharma, P.; Gupta, A.; Rao, K. V.; Owens, F. J.; Sharma, R.; Ahuja, R.; Guillen, J. M.; Johansson, B.; Gehring, G. A. Ferromagnetism Above Room Temperature in Bulk and Transparent Thin Films of Mn-Doped ZnO. *Nat. Mater.* **2003**, *2*, 673−677.

(10) Liu, Z. Q.; Lu, W. M.; Lim, S. L.; Qiu, X. P.; Bao, N. N.; Motapothula, M.; Yi, J. B.; Yang, M.; Dhar, S.; Venkatesan, T.; et al.

Reversible Room-Temperature Ferromagnetism in Nb-Doped $SrTiO_3$ Single Crystals. *Phys. Rev. B* **2013**, *87*, 220405−9(R).
(11) Márquez, A. M.; Plata, J. J.; Ortega, Y.; Fernández-Sanz, J. Structural Defects in W-Doped TiO_2 (101) Anatase Surface: Density Functional Study. *J. Phys. Chem. C* **2011**, *115*, 16970−16976.
(12) Siemons, W.; Koster, G.; Yamamoto, H.; Harrison, W. A.; Lucovsky, G.; Geballe, T. H.; Blank, D. H. A.; Beasley, M. R. Origin of Charge Density at $LaAlO_3$ on $SrTiO_3$ Heterointerfaces: Possibility of Intrinsic Doping. *Phys. Rev. Lett.* **2007**, *98*, 196802−5.
(13) Brinkman, A.; Huijben, M.; van Zalk, M.; Huijben, J.; Zeitler, U.; Maan, J. C.; van der Wiel, W. G.; Rijnders, G.; Blank, D. H. A.; Hilgenkamp, H. Magnetic Effects at the Interface Between Non-Magnetic Oxides. *Nat. Mater.* **2007**, *6*, 493−496.
(14) Henderson, B.; Imbush, G. F.; *Optical Spectroscopy of Inorganic Solids*; Oxford Science Publications: Oxford, U.K., 1989.
(15) Wertz, J. E.; Auzins, P. Crystal Vacancy Evidence from Electron Spin Resonance. *Phys. Rev.* **1957**, *106*, 484−488.
(16) Henry, M. O.; Larkin, J. P.; Imbusch, G. F. Nature of the Broadband Luminescence Center in MgO:Cr^{3+}. *Phys. Rev. B* **1976**, *13*, 1893−1902.
(17) Fairbank, M.; Klauminzer, G. K. Tetragonal-Field Splittings of Levels in MgO: Cr^{3+}. *Phys. Rev. B* **1973**, *7*, 500−510.
(18) Castelli, F.; Forster, L. S. Fluorescence ($^4T_2 \rightarrow {}^4A_2$) and Phosphorescence ($^2E \rightarrow {}^4A_2$) in MgO: Cr^{3+}. *Phys. Rev. B* **1975**, *11*, 920−8.
(19) Pilla, O.; Montagna, M.; Viliani, G.; Santucci, S. Observation of New Centers in MgO:Cr^{3+}. *Phys. Rev. B* **1980**, *21*, 4859−4862.
(20) Zakharchenya, R. I.; Kaplyanski, A. A.; Kulinkin, A. B.; Meltzer, R. S.; Feofilov, S. P. Radiative Transitions and Spectral-Hole Burning in MgO: Cr^{3+} Nanocrystals. *Phys. Solid State* **2003**, *45*, 2209−2212.
(21) Groh, D. J.; Pandey, R.; Recio, J. M. Embedded-Quantum-Cluster Study of Local Relaxations and Optical Properties of Cr^{3+} in MgO. *Phys. Rev. B* **1994**, *50*, 14860−6.
(22) Yeung, Y. Y. Superposition Model and Its Applications. In *Optical Properties of 3d-Ions in Crystals*; Avram, N. M., Brik, M. G., Eds.; Springer: Heidelberg, Germany, 2013.
(23) Powell, R. C. *Physics of Solid State Laser Materials*; Springer: New York, 1998.
(24) Garcia-Fernandez, P.; Trueba, A.; Borja-Cueto, B.; Aramburu, J. A.; Barriuso, M. T.; Moreno, M. Impurities Bound to Vacancies in Insulators: Electronic Relaxation and Physical Properties of the Cr^{3+}-V_M Model Center in KMF_3 (M = Mg, Zn). *Phys. Rev. B* **2011**, *83*, 125123−125134.
(25) Sakhabutdinova, N.; van Yperen-De Deyne, A.; Pauwels, E.; van Speybroeck, V.; Vrielinck, H.; Callens, F.; Waroquier, M. Assessment of Periodic and Cluster-in-Vacuo Models for First Principles Calculation of EPR Parameters of Paramagnetic Defects in Crystals: Rh^{2+} Defects in NaCl as Case Study. *J. Phys. Chem. A* **2011**, *115*, 1721−1733.
(26) Isseroff, L. Y.; Carter, E. A. Electronic Structure of Pure and Doped Cuprous Oxide with Copper Vacancies: Suppression of Trap States. *Chem. Mater.* **2013**, *25*, 253−265.
(27) Aramburu, J. A.; Garcia-Fernandez, P.; Garcia-Lastra, J. M.; Barriuso, M. T.; Moreno, M. Colour Due to Cr^{3+} Ions in Oxides: A Study of the Model System MgO:Cr^{3+}. *J. Phys.: Condens. Matter* **2013**, *25*, 175501−8.
(28) Dong-Ping, M.; Ellis, D. E. Optical Spectra of MgO:Cr^{3+} and MgO:V^{2+} and Their Pressure-Induced Shifts. *J. Lumin.* **1997**, *71*, 329−331.
(29) Avram, N. M.; Brik, M. G.; Kityk, I. V. Studies of Variation of Interionic Distances and Crystal Field Effects in ZnS:V^{2+} and MgO:Cr^{3+}. *Opt. Mater.* **2010**, *32*, 1668−1670.
(30) Garcia-Lastra, J. M.; Aramburu, J. A.; Barriuso, M. T.; Moreno, M. Optical Properties of Cr^{3+}-Doped Oxides: Different Behavior of Two Centers in Alexandrite. *Phys. Rev. B* **2006**, *74*, 115118−115122.
(31) Aramburu, J. A.; Garcia-Fernandez, P.; Garcia-Lastra, J. M.; Barriuso, M. T.; Moreno, M. Internal Electric Fields and Color Shift in Cr^{3+}-Based Gemstones. *Phys. Rev. B* **2012**, *85*, 245118−245127.
(32) Trueba, A.; Garcia-Fernandez, P.; García-Lastra, J. M.; Barriuso, M. T.; Aramburu, J. A.; Moreno, M. Spectrochemical Series and the Dependence of Racah and 10*Dq* Parameters on the Metal−Ligand Distance: Microscopic Origin. *J. Phys. Chem. A* **2011**, *115*, 1423−1432.
(33) Moreno, M.; Aramburu, J. A.; Barriuso, M. T. Electronic Properties and Bonding in Transition Metal Complexes: Influence of Pressure. *Struct. Bonding* **2004**, *106*, 127−152.
(34) Brik, M. G.; Kumar, G. A.; Sardar, D. K. Ab Initio, Crystal Field and Experimental Spectroscopic Studies of Pure and Ni^{2+}-Doped $KZnF_3$ Crystals. *Mater. Chem. Phys.* **2012**, *136*, 90−112.
(35) Dovesi, R.; Civalleri, B.; Orlando, R.; Roetti, C.; Saunders, V. R. Ab Initio Quantum Simulation in Solid State Chemistry. *Rev. Comput. Chem.* **2005**, *21*, 1−125.
(36) CRYSTAL Basis Sets. http://www.crystal.unito.it/Basis_Sets/Ptable.html.
(37) Perdew, J. P.; Ruzsinszky, A.; Csonka, G. I.; Vydrov, O. A.; Scuseria, G. E.; Constantin, L. A.; Zhou, X.; Burke, K. Restoring the Density-Gradient Expansion for Exchange in Solids and Surfaces. *Phys. Rev. Lett.* **2008**, *100*, 136406−9.
(38) Bilc, D. I.; Orlando, R.; Shaltaf, R.; Rignanese, G.-M.; Iñiguez, J.; Ghosez, P. Hybrid Exchange-Correlation Functional for Accurate Prediction of the Electronic and Structural Properties of Ferroelectric Oxides. *Phys. Rev. B* **2008**, *77*, 165107−165119.
(39) te Velde, G.; Bickelhaupt, F. M.; Baerends, E. J.; Guerra, C. F.; van Gisbergen, S. J. A.; Snijders, J. G.; Ziegler, T. Chemistry with ADF. *J. Comput. Chem.* **2001**, *22*, 931−967.
(40) Atanasov, M.; Daul, C. A.; Rauzy, C. New Insights into the Effects of Covalency on the Ligand Field Parameters: a DFT Study. *Chem. Phys. Lett.* **2003**, *367*, 737−746.
(41) Perdew, J. P. *Electronic Structure of Solids '91*; Ziesche, P., Eschrig, H., Eds.; Akademie Verlag: Berlin, Germany, 1991; p 11.
(42) Moreno, M.; Barriuso, M. T.; Aramburu, J. A.; Garcia-Fernandez, P.; Garcia-Lastra, J. M. Microscopic Insight into Properties and Electronic Instabilities of Impurities in Cubic and Lower Symmetry Insulators: the Influence of Pressure. *J. Phys.: Condens. Matter* **2006**, *18*, R315−R360.
(43) Binois, M.; Leble, A.; Rousseau, J. J.; Fayet, J. C. Point Defects of Low Symmetry in $KZnF_3$ Single Crystals. *J. Phys., Colloq.* **1973**, *34*, 285−7.
(44) Watkins, G. D. Electron Spin Resonance of Mn^{+2} in Alkali Chlorides: Association with Vacancies and Impurities. *Phys. Rev.* **1958**, *113*, 79−90.
(45) Lopez, F. J.; Jaque, F. J. EPR Study of the Relative Stabilities of Dipoles in NaCl: Mn^{+2}. *J. Phys. Soc. Jpn.* **1974**, *37*, 1466.
(46) Trueba, A.; Garcia-Lastra, J. M.; Garcia-Fernandez, P.; Barriuso, M. T.; Aramburu, J. A.; Moreno, M. Cr^{3+}-Doped Fluorides and Oxides: Role of Internal Fields and Limitations of the Tanabe−Sugano Approach. *J. Phys. Chem. A* **2011**, *115*, 13399−13406.
(47) Kohn, W. Density Functional and Density Matrix Method Scaling Linearly with the Number of Atoms. *Phys. Rev. Lett.* **1996**, *76*, 3168−3171.
(48) Garcia-Fernandez, P.; Barriuso, M. T.; García-Lastra, J. M.; Moreno, M.; Aramburu, J. A. Compounds Containing Tetragonal Cu^{2+} Complexes: Is the $d_{x^2-y^2}$−$d_{3z^2-r^2}$ Gap a Direct Reflection of the Distortion? *J. Phys. Chem. Lett.* **2013**, *4*, 2385−2390.
(49) Reinen, D. The Modulation of Jahn−Teller Coupling by Elastic and Binding Strain Perturbations: A Novel View on an Old Phenomenon and Examples from Solid-State Chemistry. *Inorg. Chem.* **2012**, *51*, 4458−4472.
(50) Aramburu, J. A.; García-Lastra, J. M.; García-Fernández, P.; Barriuso, M. T.; Moreno, M. Cu^{2+} in Layered Compounds: Origin of the Compressed Geometry in the Model System K_2ZnF_4:Cu^{2+}. *Inorg. Chem.* **2013**, *52*, 6923−6933.